



Cite this: *RSC Chem. Biol.*, 2025, 6, 1616

## Characterization of nuclease stability and poly(A)-binding protein binding activity of chemically modified poly(A) tail for *in vivo* applications

Atsushi Hashimoto, <sup>a</sup> Yuma Kunitomo, <sup>a</sup> Ittoku Kikuchi, <sup>a</sup> Hiroki Yamada, <sup>a</sup> Keiko Kobayashi, <sup>a</sup> Kazuhiro Soshiroda, <sup>a</sup> Hiromi Aman, <sup>a</sup> Yasuaki Kimura, <sup>d</sup> Junichiro Yamamoto, <sup>a</sup> Yasuhisa Shiraishi, <sup>a</sup> Satoshi Uchida, <sup>\*bc</sup> Hiroshi Abe <sup>\*defg</sup> and Hiroto Iwai <sup>\*a</sup>

The poly(A) tail plays a crucial role in mRNA stability and translation efficiency. Chemical modification of the poly(A) tail is a promising approach for stabilizing mRNA against deadenylation. In this study, we investigated the effect of poly(A) chemical modifications using phosphorothioate (PS), 2'-fluoro (2'-F), 2'-O-methyl (2'-OMe), and 2'-O-methoxyethyl (2'-MOE) modifications. Notably, PS, 2'-OMe, and 2'-MOE modifications conferred resistance to CAF1, an enzyme responsible for deadenylation. Interestingly, only the PS modification retained the poly(A)-binding protein (PABP) binding activity, which is critical for translation, whereas 2'-F, 2'-OMe, and 2'-MOE modifications abolished this activity. Beyond the PS modification, the combination of 2'-F, 2'-OMe, and 2'-MOE modifications resulted in enhanced resistance to both CAF1 and other nucleases. Based on these results, a 12-nucleotide unmodified poly(A) sequence was inserted upstream of the modified poly(A) to confer both nuclease resistance and PABP-binding activity. Notably, the resulting poly(A) formulation significantly prolonged protein expression in cultured cells and mouse skin when applied to epidermal growth factor-encoding therapeutic mRNA. Collectively, this study presents a design concept for poly(A) chemical modifications to achieve durable protein expression from mRNA, offering a promising strategy for enhancing the function of mRNA-based therapeutics.

Received 30th May 2025,  
Accepted 17th August 2025

DOI: 10.1039/d5cb00137d

[rsc.li/rsc-chembio](http://rsc.li/rsc-chembio)

### Introduction

Despite the successful clinical application of mRNA vaccines and therapeutics, their transient protein expression profile hinders their widespread use.<sup>1,2</sup> For instance, mRNA-based protein replacement therapy requires repeated administration,

highlighting the need for strategies that prolong protein expression.<sup>3,4</sup> Engineering the poly(A) tail is a promising solution.<sup>5,6</sup> The poly(A) tail is a critical mRNA element that contributes significantly to mRNA stability, translation efficiency, and overall gene expression regulation in eukaryotic cells.<sup>6–9</sup> The poly(A) tail is added to the 3'-end of the mRNA during posttranscriptional processing and covered by poly(A)-binding protein (PABP).<sup>10–12</sup> These interactions facilitate the formation of a closed-loop structure mediated by the interaction between the 5'-cap structure and poly(A) tail.<sup>13,14</sup> This closed-loop structure plays an important role in protecting mRNA from exonucleolytic degradation and facilitates the recruitment of ribosomes for translation initiation.<sup>15,16</sup>

Recent advancements in transcriptome analysis and RNA engineering have revealed that stabilization of the poly(A) tail is a promising approach for increasing mRNA durability.<sup>5,6,17</sup> Chemical modifications of RNA provide a robust tool for enhancing its enzymatic and physiological stability, as demonstrated by the development of oligonucleotide therapeutics.<sup>18,19</sup> Although RNA modifications in the 2'-position have been

<sup>a</sup> Innovation Center, Research Division, Kyowa Kirin Co., Ltd. 3-6-6 Asahi, Machida, Tokyo, 194-8533, Japan. E-mail: [hiroto.iwai.sk@kyowakirin.com](mailto:hiroto.iwai.sk@kyowakirin.com)

<sup>b</sup> Department of Advanced Nanomedical Engineering, Medical Research Laboratory, Institute of Integrated Research, Institute of Science Tokyo, 1-5-45 Yushima, Bunkyo-ku, Tokyo, 113-8510, Japan

<sup>c</sup> Innovation Center of NanoMedicine (iCONM), Kawasaki Institute of Industrial Promotion, Kawasaki, Japan

<sup>d</sup> Department of Chemistry, Graduate School of Science, Nagoya University, Furo, Chikusa, Nagoya 464-8602, Japan

<sup>e</sup> Research Center for Materials Science, Nagoya University, Furo, Chikusa, Nagoya 464-8602, Japan

<sup>f</sup> CREST, Japan Science and Technology Agency, 7, Gobancho, Chiyoda-ku, Tokyo 102-0076, Japan

<sup>g</sup> Institute for Glyco-core Research (iGCORE), Nagoya University, Furo-cho, Chikusa-ku, Nagoya, Aichi 464-8601, Japan



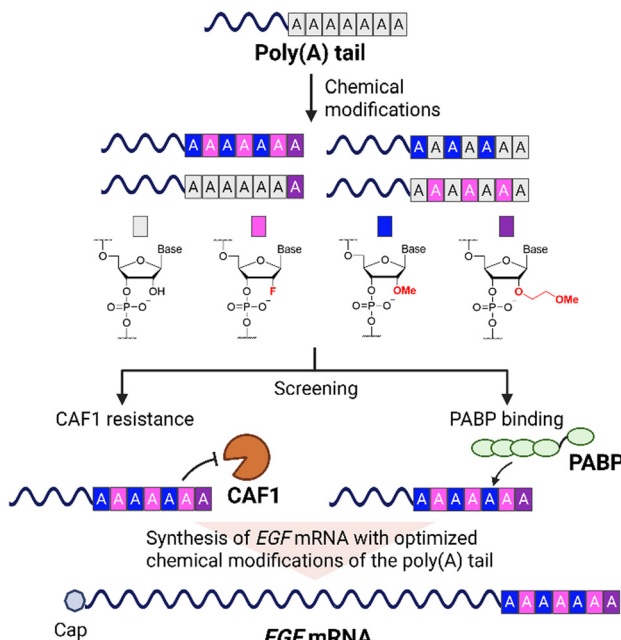


**Fig. 1** Concept of this study. Poly(A) tails with chemical modifications were chemically synthesized. The stability against CAF1 and PABP binding affinity was evaluated for each poly(A) tail. Chemical modifications that confer both CAF1 resistance and PABP binding affinity were selected, and EGF mRNA with optimized modifications was synthesized and evaluated *in vivo*. Created in BioRender. Hashimoto, A. (2025) <https://BioRender.com/pbs5is8>.

widely tested, the stabilizing effects largely depend on the modification type.<sup>18,19</sup> For example, 2'-O-methyl (OMe)-RNA showed higher stability against snake venom phosphodiesterase and S1 nuclease compared with 2'-fluoro (F)-RNA, with 2'-F-RNA being more stable than 2'-hydroxy (OH)-RNA.<sup>20</sup> Recent studies have addressed the poly(A) modifications of mRNAs and successfully prolonged protein expression using phosphorothioate (PS)-RNA, O-methoxyethyl (MOE)-RNA, and a 3'-linkage of inverted-2'-deoxythymidine at the 3'-end of the poly(A) tail.<sup>5,6,17</sup> However, in most cases, only a few residues at the 3'-end of the mRNA were chemically modified, leaving the effects of modifications on longer poly(A) sequences unclear. Furthermore, the optimal chemical modification type remains uncertain because of the lack of comprehensive head-to-head comparisons between different poly(A) tail modifications.

In this study, we evaluated the effect of chemical modifications of the poly(A) tail, especially at high modification rates, based on two key factors: nuclease resistance, particularly against CAF1, and PABP-binding activity (Fig. 1). We focused on sugar rather than base modifications because the commonly used adenine base modification, *N*<sup>6</sup>-methyladenosine, failed to increase the stability against CAF1.<sup>21</sup> In addition, previous studies have revealed the benefit of sugar modifications in poly(A) stabilization.<sup>6,17</sup> The comparison among PS, 2'-F, 2'-OMe, and 2'-MOE modifications identified PS modification as a promising candidate, as it inhibited degradation by CAF1 while preserving PABP binding. Considering some drawbacks

of PS modification in the synthetic context, we explored other formulations, observing that combinational modification with 2'-F, 2'-OMe, and 2'-MOE exhibited high resistance to CAF1 and other nucleases. Although 2'-F, 2'-OMe, and 2'-MOE modifications did not show clear binding affinity, this combinational modification regained PABP binding when a 12-nucleotide (nt) unmodified poly(A) was inserted upstream of the modified poly(A) sequence, even at a 100% modification rate in the 28-nt poly(A) sequence at the 3'-end. Ultimately, the modification successfully prolonged the translation of epidermal growth factor (EGF) from EGF mRNA in mouse skin for up to 1 week, showing promise for future therapeutic applications to skin ulcers.

## Results and discussion

### Nuclease resistance of chemically modified poly(A) tail

To investigate the effect of chemical modifications on resistance to deadenylation, we focused on CAF1, a catalytic subunit of the CCR4-NOT deadenylase complex.<sup>22,23</sup> Therefore, we conducted *in vitro* degradation assays using recombinant CAF1 on 5'-ATTO488-labeled RNA substrates. Each RNA substrate consisted of 13-nt unmodified nonpoly(A) RNA, 20-nt unmodified poly(A), and 20-nt poly(A) with various chemical modifications from the 5' to 3'-end (Fig. 2A). The SI (Table S1) lists the design and sequences of the RNA substrates. Regarding the modification rates used in this assay, previous studies showed the benefit of increasing the rates in enhancing mRNA

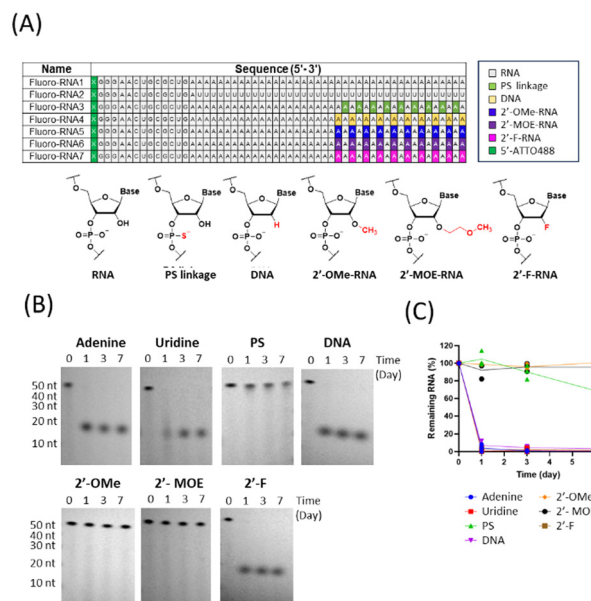


**Fig. 2** *In vitro* stability of RNA fragments against CAF1. (A) Design and sequences of RNA fragments with chemical modifications. (B) TBE-urea gel image of RNA fragments after CAF1 treatment. Experiments were performed using biological triplicates and representative data are shown. (C) Time course of the remaining RNA ratio after incubation with CAF1. Data are presented as the mean. Blue: fluoro-RNA1, red: fluoro-RNA2, green: fluoro-RNA3, purple: fluoro-RNA4, orange: fluoro-RNA5, black: fluoro-RNA6, brown: fluoro-RNA7.



stability.<sup>6,17</sup> However, almost complete modification of the poly(A) tail drastically reduced the affinity for PABP, revealing the trade-off relationship between stability improvement and PABP binding efficiency after poly(A) modification.<sup>21</sup> Based on these studies, we decided to start with a 50% modification rate.

In stability tests against CAF1, we employed denaturing polyacrylamide gel electrophoresis to quantify the remaining RNA. We used a CAF1 concentration of 2.5  $\mu$ M, which is close to that used in previous studies.<sup>24–26</sup> Previous kinetic analyses have shown that CAF1 concentrations  $<0.4$   $\mu$ M exhibit minimal deadenylation activity depending on substrate concentration.<sup>24</sup> Accordingly, we expected that the concentration of 2.5  $\mu$ M will ensure the robustness of this assay. Notably, our experiments revealed clear differences in the efficacy of chemical modifications against CAF1 degradation. We observed that PS, 2'-MOE, and 2'-OMe modifications provided significantly higher stability against CAF1 (Fig. 2B and C). These findings aligned with previous research showing that PS and 2'-OMe modifications of the poly(A) tail provide CAF1 resistance.<sup>21</sup> Although the previous study showed that 2'-F modification provides a similar resistance level as 2'-OMe, we did not observe any enhancement in the stability for 2'-F and DNA modifications (Fig. 2B and C). This difference may be attributed to the higher CAF1 concentration used in our study (2.5  $\mu$ M) compared with that in the previous study (approximately 0.15 nM), which may lead to the degradation of 2'-F modified poly(A). Further experiments, including those examining the CAF1 dose-dependency, are necessary to clarify the discrepancies between the present and previous findings. Overall, our study revealed that bulky structures such as 2'-MOE and 2'-OMe in the 2'-position of RNA are generally effective at providing CAF1 resistance. Although 2'-F conferred some degree of protection, its efficacy was limited relative to the more structurally bulky modifications.

#### Binding activity of PABP to chemically modified poly(A) tail

PABP is an essential factor for eukaryotic translation.<sup>12,27</sup> PABP consists of four N-terminal RRM domains (RRM1–4), a proline-rich linker, and a C-terminal MLLE domain.<sup>28,29</sup> To assess the binding activity of PABP to the poly(A) tail, we used surface plasmon resonance (SPR). We immobilized the 5'-biotin labeled A24 with chemical modifications onto a streptavidin-coated sensor chip, and measured the response rate for PABP binding (Fig. 3A and Table S2). The full-length of PABP was used in this study. The  $K_D$  value for PABP to unmodified A24 was 0.02 nM (Fig. 3B and Table 1), compared to a  $K_D$  value of 0.7 nM in the previous study,<sup>30</sup> indicating a 35-fold higher binding affinity in our study. This higher affinity may be attributed to a positively charged His-tag used in our study, which probably strengthened the binding affinity for the negatively charged A24.

Regarding the chemically modified poly(A) tail, the PS modification led to a 1.8-fold increase in affinity compared with unmodified poly(A) (Fig. 3B and Table 1). In contrast, we did not detect any binding response for DNA, 2'-OMe, 2'-MOE, and 2'-F modified A24 (Fig. 3B). Notably, the previous study<sup>21</sup> revealed that PABP with a single substitution to 2'-F or 2'-OMe

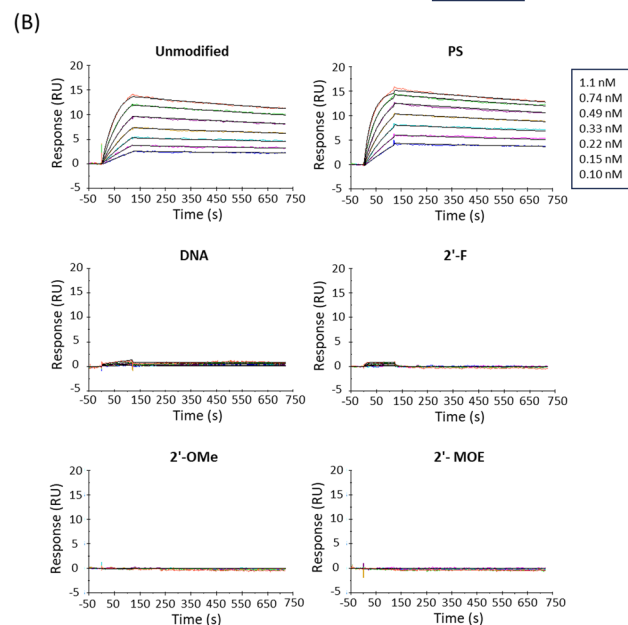
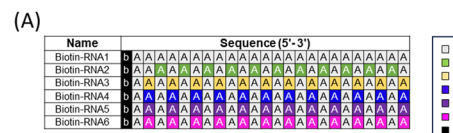


Fig. 3 SPR analysis of chemically modified poly(A) tails. (A) Design and sequences of poly(A) tails with chemical modifications. (B) SPR sensorgrams of interactions between PABP and poly(A) tails. Black lines represent the 1:1 binding model. Experiments were performed using biological triplicates and representative data are shown. The  $K_D$  values determined through this SPR analysis are shown in Table 1.

in the middle position of A12 still bound to RNA, though the affinity was decreased by four-fold for the 2'-F modification and by seven-fold for the 2'-OMe modification. In addition, in our study, 50% substitution of 2'-F or 2'-OMe in the poly(A) tail completely suppressed the PABP binding to the poly(A) tail, highlighting the importance of the modification ratio. Surprisingly, PABP still bound to a 24-nt PS-modified poly(A) tail even at a substitution rate of 46%. Overall, the PS modification prevented CAF1-mediated degradation while maintaining PABP binding affinity.

#### Nuclease stability and PABP binding activity of highly modified poly(A) tail

Although the PS modification imparts both CAF1 resistance and PABP-binding affinity, potential oxidative desulfurization that could occur during chemical synthesis may raise concerns.<sup>31,32</sup> This motivated us to explore effective modification patterns beyond the PS modification (Fig. 4A). Herein, we focused on a combinational poly(A) modification with 2'-F and 2'-OMe along with 2'-MOE modification at the last 3-nt of poly(A) (F/OMe/MOE), which previously showed high stability and translational activity in human cells.<sup>33,34</sup> In the present study, we evaluated the effects of combinational modifications on nuclease stability nucleases and PABP binding affinity.



Table 1 Kinetics parameters obtained via SPR analysis of PABP-poly(A) interaction

Name	Length (nt)	Modification	$k_a$ ( $M^{-1} s^{-1}$ )	$k_d$ ( $s^{-1}$ )	$K_D$ (M)
Biotin-RNA1	24	—	$2.3 \pm 0.2 \times 10^7$	$3.9 \pm 0.4 \times 10^{-4}$	$1.7 \pm 0.1 \times 10^{-11}$
Biotin-RNA2	24	PS	$3.2 \pm 0.1 \times 10^7$	$2.8 \pm 0.1 \times 10^{-4}$	$9.2 \pm 0.7 \times 10^{-12}$
Biotin-RNA3	24	DNA	n.b.	n.b.	n.b.
Biotin-RNA4	24	2'-OMe	n.b.	n.b.	n.b.
Biotin-RNA5	24	2'-MOE	n.b.	n.b.	n.b.
Biotin-RNA6	24	2'-F	n.b.	n.b.	n.b.
Biotin-RNA7	50	—	$1.6 \pm 0.1 \times 10^7$	$2.3 \pm 0.1 \times 10^{-4}$	$1.5 \pm 0.2 \times 10^{-11}$
Biotin-RNA8	50	U	n.b.	n.b.	n.b.
Biotin-RNA9	50	2'-F, 2'-OMe, 2'-MOE	$3.0 \pm 0.4 \times 10^7$	$1.5 \pm 0.1 \times 10^{-2}$	$5.0 \pm 0.4 \times 10^{-10}$
Biotin-RNA10	12	—	n.d.	n.d.	$1.5 \pm 0.1 \times 10^{-7}$

Each experiment was repeated using biological triplicates and the mean values are listed. The binding affinity of biotin-RNA10 was determined using a steady-state affinity 1:1 binding model because the sensorgram was box-shaped. n.b.: no binding, n.d.: not determined.

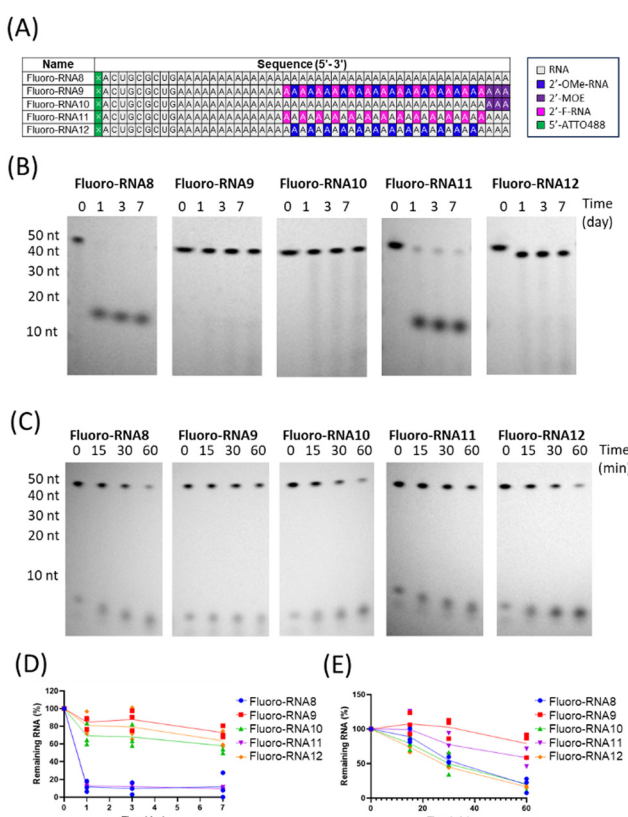


Fig. 4 *In vitro* stability of highly chemically modified RNA fragments. (A) Design of RNA fragments with chemical modifications. (B) TBE-urea gel image of RNA fragments after CAF1 treatment. Experiments were performed using biological triplicates and representative data are shown. (C) TBE-urea gel image of RNA fragments after treatment of mouse skin lysates. Experiments were performed using biological triplicates and representative data are shown. (D) Time course of the remaining RNA ratio after incubation with CAF1. Data are presented as the mean. (E) Time course of the remaining RNA ratio after incubation with mouse skin lysates. Data are presented as the mean.

Furthermore, to gain a deeper understanding of the individual contributions of these modifications, we prepared control RNA species containing only one of the three tested modifications: fluoro-RNA10 for 2'-MOE, fluoro-RNA11 for 2'-F, and fluoro-RNA12 for 2'-OMe. In the CAF1 assay, F/OMe/MOE

modifications imparted mRNAs with high stability, exhibiting undetectable degradation, even after 1 week of incubation (fluoro-RNA9; Fig. 4B and D). Notably, the 3-nt 2'-MOE modification at the 3'-end completely blocked CAF1 degradation even without upstream 2'-F and 2'-OMe modifications (Fig. 4B and D). This result indicated that the 3'-end 2'-MOE modification of poly(A) is sufficient to inhibit deadenylation, consistent with the findings of previous studies.<sup>25</sup> Concurring with the results in Fig. 1, 2'-F modifications alone did not increase the resistance to CAF1 (fluoro-RNA11; Fig. 4B and D). 2'-OMe modifications resulted in the degradation of the unmodified four bases at the 3'-end, leaving the upstream modified sequence intact (fluoro-RNA12; Fig. 4B and D). This result supported the findings in Fig. 1, showing the high stability against CAF1 resulting from the 2'-OMe modification.

mRNA is degraded not only by CAF1 but also by other nucleases.<sup>35</sup> To evaluate the overall stability against various nucleases, we assessed the stability of the poly(A) tail in mouse skin lysates. We used mouse skin lysates because the subsequent *in vivo* studies were performed using mouse skin samples. After incubating 5'-fluorescently labeled RNA substrates with diluted skin lysates, we subjected the reaction mixtures to denaturing polyacrylamide gel electrophoresis. Importantly, the experimental groups differed only in the composition of modified adenosine residues. Therefore, any differences observed between groups can be attributed to the effects of the specific modification compositions. We first compared poly(A) with poly(U) and found that poly(U) degraded faster than poly(A) (Fig. S1). This result aligned with previous studies indicating that ribonuclease activity on the mouse skin surface is pyrimidine selective.<sup>36</sup> We then assessed the chemically modified poly(A) tails and found that F/OMe/MOE modifications resulted in highly stable mRNAs in mouse skin lysates (fluoro-RNA9; Fig. 4C and E). Upon studying the contribution of each modification separately, we noted that 2'-F modifications (fluoro-RNA11) but not 2'-OMe or terminal 2'-MOE modifications (fluoro-RNA10 and 12) increased nuclease stability compared with unmodified poly(A) (fluoro-RNA8) (Fig. 4C and E).

Interestingly, we observed that each modification exhibited different preferences for preventing degradation by specific types of nucleases, with 2'-OMe and 2'-MOE modifications



providing resistance to CAF1, whereas the 2'-F modification providing resistance to nucleases in skin lysates. This highlights the potential benefits of combined modifications in protecting RNA from various types of nucleases. These results indicated that the modification rate is crucial for enhancing the stability of the poly(A) tail against a variety of nucleases.

Next, we evaluated the binding affinity of PABP to the poly(A) tail with F/OMe/MOE modifications. Based on our results (Fig. 3), we expected this modification to suppress PABP binding to RNA. To address this issue, we inserted 12 bases of unmodified poly(A) upstream of the (A12-F/OMe/MOE)-modified poly(A) tail. We set the length of the unmodified poly(A) to 12-nt because PABP requires A11 to A12 for minimal binding activity.<sup>37</sup> We assessed the binding affinity of PABP to A12-F/OMe/MOE using SPR. Notably, A12-F/OMe/MOE was still capable of binding to PABP even at a 100% modification rate in the 28-nt poly(A) sequence at the 3' end (Fig. 5A, B and Table 1). Although the  $K_D$  value for A12-F/OMe/MOE was 34-fold lower than that for unmodified poly(A) (A40), this affinity is likely sufficient for PABP to bind to the poly(A) tail, considering that the intracellular concentration of PABP is at the micromolar level.<sup>38</sup> The partial recovery of PABP binding affinity may be attributed to the fact that four RRM<sub>s</sub> require a 24-nt poly(A) sequence, whereas A12 interacts with only two RRM<sub>s</sub>.<sup>11</sup>

Interestingly, A12-F/OMe/MOE showed 291-fold higher affinity than A12 (Fig. 5A, B and Table 1). This result suggested that PABP could still bind to the F/OMe/MOE region, although 2'-F, 2'-OMe, and 2'-MOE decreased the binding affinity of PABP to the poly(A) tail.

In conclusion, A12-F/OMe/MOE imparted the mRNA with high stability against both CAF1 and mouse skin lysates while maintaining sufficient PABP-binding activity. Based on these

results, we used this formulation in subsequent functional studies involving cultured cells and animals.

### Synthesis of EGF mRNA with modified poly(A) tail

To evaluate the effects of A12-F/OMe/MOE modifications on therapeutic mRNAs, we synthesized a modified mRNA encoding EGF. EGF is a polypeptide consisting of 53 amino acids that stimulates the growth and differentiation of epithelial cells.<sup>39-41</sup> Previous studies have demonstrated that EGF can accelerate wound healing and is a promising drug candidate for the treatment of skin ulcers.<sup>42,43</sup> Despite its potential, EGF has a short half-life of approximately 2–7 h, which limits its therapeutic efficacy.<sup>42,44,45</sup> The use of mRNA may improve the therapeutic potential of EGF by continuously providing EGF protein to skin lesions, and poly(A) modifications are expected to further enhance this benefit by prolonging EGF expression.

We designed EGF mRNA with F/OMe/MOE modifications on the poly(A) tail (EGF mRNA\_Mod) and EGF mRNA without poly(A) tail modification (EGF mRNA\_Unmod) as a control (Fig. 6A). We introduced the Cap1 structure at the 5'-end of these two mRNAs to minimize the immune reaction and improve translation activity *in vivo*.<sup>46</sup> Instead of using *in vitro* transcription (IVT), a widely used method for mRNA preparation and employed in clinically approved SARS-CoV-2 mRNA vaccines,<sup>47</sup> we chemically synthesized mRNAs. Solid-phase chemical synthesis offers an easier approach for site-specific sugar modifications in RNA strands than the IVT method.<sup>48,49</sup>

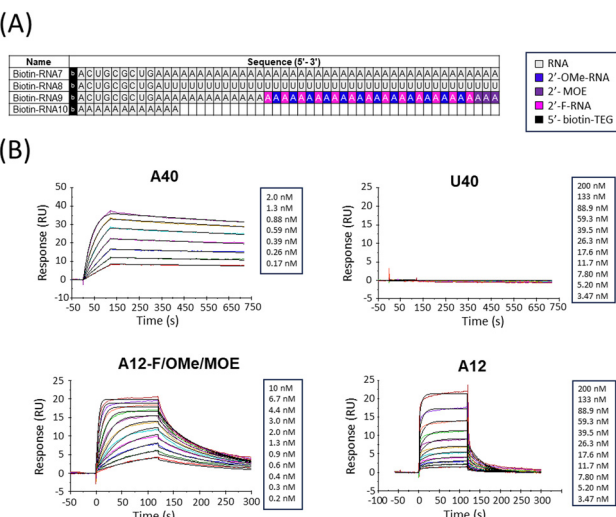


**Fig. 5** SPR analysis of poly(A) tails with extensive chemical modifications. (A) Design of poly(A) tails with chemical modifications. (B) SPR sensorgrams of interactions between PABP and poly(A) tails. Black lines represent the 1:1 binding model. Experiments were performed using biological triplicates and representative data are shown. The  $K_D$  values determined through this SPR analysis are shown in Table 1.

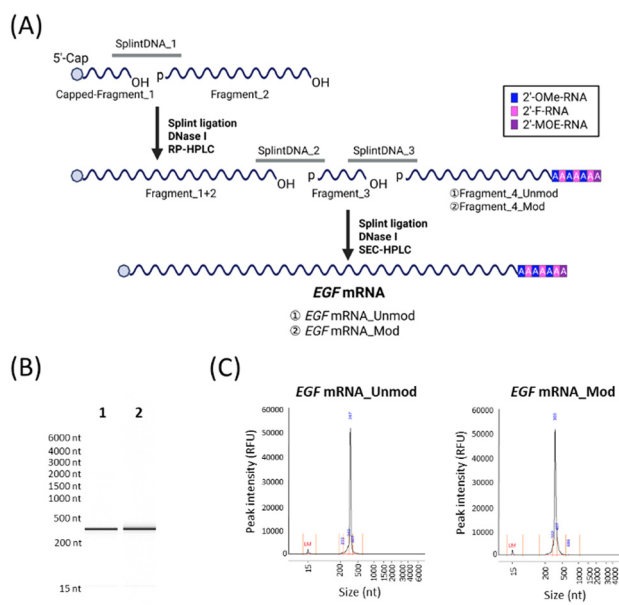


**Fig. 6** Synthesis and analysis of EGF mRNAs. (A) Schematic view of splint ligation. After splint ligation and DNase I treatment, Fragment\_1 + 2 was purified using reverse-phase HPLC (RP-HPLC), whereas EGF mRNAs were purified using size exclusion chromatography HPLC (SEC-HPLC). 5'-Cap = 7-methyl guanosine cap structure, p = phosphate, OH = hydroxide. (B) and (C) Results of capillary gel electrophoresis of EGF mRNAs. 1; EGF mRNA\_Unmod, 2; EGF mRNA\_Mod. Y-Axis shows the intensity of the relative fluorescence units and X-axis shows RNA size. Created in BioRender. Hashimoto, A. (2025) <https://BioRender.com/z8prx78>.

Although the chemical synthesis of long RNA strands is challenging, the splint ligation of short RNA fragments helps avoid this issue. Indeed, we previously reported the chemical synthesis of mRNA with extensive sugar modifications using splint ligation.<sup>33</sup> Additionally, a subsequent chemical capping reaction enables complete chemical synthesis of mRNA.<sup>46</sup> We synthesized the EGF mRNAs using T4 RNA ligase 2 through convergent splint ligation with the corresponding RNA fragments (Fig. 6A). The details of the synthesis results are described in the SI. Notably, the purified mRNAs were homogeneous in length, showing a single peak on PAGE and capillary gel electrophoresis (Fig. 6B, C and Fig. S6). Splint DNA digestion was confirmed using denaturing PAGE, as previously described<sup>34</sup> (Fig. S5).

### Poly(A)-modified EGF mRNA showed prolonged translational activity

First, we evaluated the effects of chemical modifications of the poly(A) tail in HeLa cells, a human cell line. After treating HeLa cells with lipid-based carriers loaded with EGF mRNA, we measured EGF protein concentrations in the culture medium. After each measurement, we replaced the medium with fresh medium. Interestingly, the benefit of poly(A) tail modifications became obvious only at a later time point, potentially reflecting their mRNA stabilizing effect (Fig. 7A). Specifically, poly(A)-modified mRNA resulted in the production of a higher concentration of EGF than the unmodified mRNA at 48 h after mRNA addition, but not at 6 and 24 h. At 6 h, poly(A)-modified mRNA resulted in lower EGF levels than unmodified mRNA, possibly

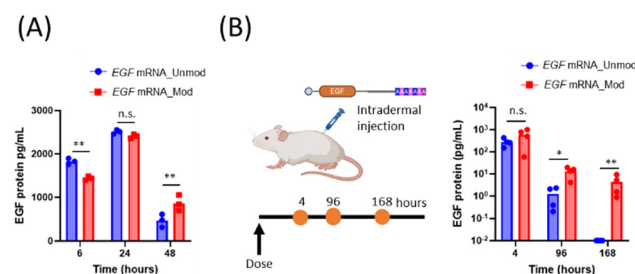


**Fig. 7** *In vitro* and *in vivo* stability of EGF-mRNA with chemical modifications on the poly(A) tail. (A) Time course of EGF protein concentration secreted from HeLa cells. Bars indicate mean values. The tests were performed in biological triplicates. Blue: EGF-mRNA\_Unmod, red: EGF-mRNA\_Mod. Statistical analysis between the two samples was performed using Šídák multiple comparison test. Untreated and mock wells containing the transfection reagent without mRNAs were prepared as negative controls. The protein levels were either at background level or below the lower limit of quantitation (LLOQ). (B) Relative EGF protein levels in mice skin lysates. The vertical axis shows EGF protein concentration normalized by total protein level on a log scale. The tests were performed in biological quadruplicates. Statistical analysis between the two samples was performed using Šídák multiple comparison test. Dots indicate measurements for each individual mouse and bars indicate mean values. Blue: EGF-mRNA\_Unmod, red: EGF-mRNA\_Mod. The protein level was at LLOQ in mice treated with citrate–saline buffer (10 mM citrate, 130 mM NaCl pH 7.5) used as negative control.<sup>51</sup> (A) and (B), Statistical differences: n.s.,  $p > 0.05$ ; \* $p < 0.05$ ; \*\* $p < 0.01$ ; \*\*\* $p < 0.001$ . Created in BioRender. Hashimoto, A. (2025) <https://BioRender.com/zc59z61>.

because of the lower affinity of PABP for poly(A)-modified mRNA (Fig. 5).

Next, we explored the *in vivo* delivery of poly(A)-modified mRNA to the skin, as EGF mRNA is a promising candidate for treating skin ulcers. As a delivery method, we selected naked mRNA injection using a needle-free pyro-drive liquid jet injector (PYRO), which facilitates the penetration of mRNA through the cell membrane into skin cells *via* physical pressure.<sup>50</sup> To confirm the effect of PYRO, naked luciferase mRNA was injected into mice using either a needle and syringe (N&S) or PYRO, followed by luminescence intensity measurements 4 h after injection. We found that PYRO improved luminescence intensity by 11-fold at a dose of 10  $\mu$ g per head and 16-fold at a dose of 30  $\mu$ g per head compared with N&S (Fig. S2). These data corroborate previous studies showing the benefits of PYRO for naked mRNA delivery to the skin.<sup>50</sup>

Finally, we assessed the *in vivo* activity of poly(A)-modified EGF mRNA (Fig. 7B). For this purpose, we administered EGF mRNA intradermally using PYRO, followed by continuous measurement of EGF protein concentration in the skin. Although EGF expression levels were comparable between poly(A)-modified and unmodified mRNAs at 4 h postinjection, poly(A)-modified mRNA showed enhanced expression at 96 and 168 h. Strikingly, poly(A)-modified EGF mRNA exhibited extended protein expression for up to 1 week, whereas unmodified mRNA showed no detectable protein expression at that time point (Fig. 7B).

In summary, our data showed that poly(A) tail modifications significantly enhanced protein expression *in vivo*, which is likely due to the enhanced stability of the poly(A)-modified mRNA. Prolonged EGF expression could benefit future applications of EGF mRNA therapeutics in the treatment of skin ulcers. We are planning a future study that will include therapeutic application testing and a comprehensive analysis of the *in vivo* functionality of poly(A)-modified mRNA, including expression kinetics and total protein output.

## Experimental

### Preparation of recombinant hCAF1 and hPABP

The vectors used to express hCAF1 and hPABP in our study, pET-28a(+)-HIS8/SUMO3/TEV/CAF1 and pCS-6xHis/TEV/hPABP1 [NM\_002568.4] respectively, were constructed and packaged by VectorBuilder Inc. (Chicago, IL, USA). Detailed information about these vectors can be retrieved from <https://www.vectorbuilder.com> using the vector IDs, VB221023-1216mte and VB231222-2539wqp. Proteins were expressed in *E. coli* BL21 (DE3) Star cells (Invitrogen, Thermo Fisher Scientific, Carlsbad, CA, USA). Protein expression was induced with 1 mM IPTG when OD600 reached approximately 0.5. To obtain CAF1, cells were further cultured for approximately 20 h at 22 °C. Cell pellets were lysed with B-PER (Thermo Fisher Scientific, Waltham, MA, USA), and the proteins in the supernatant were purified using the cComplete™ His-Tag Purification Resin (Roche, Basel, Switzerland). Purified proteins were desalting with NAP-25 (Cytiva, Marlborough, MA, USA), and the SUMO tag was cleaved with



TEV protease (Promega, Madison, WI, USA). The remaining SUMO tag was removed using the cComplete™ His-Tag Purification Resin, followed by purification in a Superdex 200 Increase GL 10/300 column (Cytiva, Marlborough, MA, USA). To obtain PABP, cells were cultured for approximately 20 h at 15 °C after IPTG stimulation. Cell pellets were lysed using B-PER supplemented with 125 U per mL benzonase (Merck & Co., Inc., Rahway, NJ, USA). PABP-bound nucleic acids were digested with benzonase and further removed by 0.1% (v/v) poly (ethyleneimine) treatment (Nacalai, Kyoto, Japan). The proteins were treated with the cComplete™ His-Tag Purification Resin, followed by purification in a Superdex 200 Increase GL 10/300 column. The His-tag was retained because removal *via* TEV protease digestion followed by purification using the cComplete™ His-Tag Purification Resin resulted in a substantial decrease in protein yield.

#### *In vitro* deadenylation assay

The 5'-end of substrate RNAs was labeled with ATTO488. All fluorescently labeled oligonucleotides were purchased from Gene Design (Osaka, Japan). The stability of CAF1 was assessed as follows: 250 nM RNA fragments were mixed with 2.5 μM CAF1 in a reaction buffer (20 mM Tris-HCl, 150 mM NaCl, 5 mM MgCl<sub>2</sub>, and 1 mM DTT pH 8.0) at 37 °C. At each time point, TBE-urea sample buffer (Thermo Fisher Scientific) was added to the reaction mixture to stop the degradation. The reaction products were resolved on 10% Novex TBE-urea gels (Thermo Fisher Scientific). The gel was visualized using an LAS-3000 system (Fujifilm, Tokyo, Japan), and band intensities were measured using the Multi Gauge V3.0 software (Fujifilm). The stability against mouse skin lysates was assessed using the same method. Briefly, 250 nM RNA fragments were mixed with 0.8% mouse skin lysates, and the reaction products were resolved on 15% Novex TBE-urea Gels.

#### Surface plasmon resonance (SPR)

The SPR binding assay was performed using a Biacore T200 system (GE Healthcare, Chicago, IL, USA). The 5'-biotinylated RNA fragments were captured on a streptavidin-coated sensor chip (GE Healthcare) in running buffer (10 mM HEPES, 600 mM NaCl, 3 mM EDTA, and 0.005% v/v surfactant P20 pH 7.4). A flow cell in which the RNA fragments were not captured was used as a reference cell. All experiments were conducted at 25 °C at a flow rate of 30 μL min<sup>-1</sup>. To measure PABP binding to A24 and A40, PABP was injected for 2 min and allowed to dissociate for 10 min. For A12, the dissociation time was 3 min. The surface was regenerated using 0.1% SDS for 2 min. The dataset was fitted with a 1:1 binding model and the kinetic parameters were determined.

#### Oligonucleotides

Oligonucleotides used for the *in vitro* deadenylation assay and SPR were purchased from Gene Design. The RNA fragments used for chemical synthesis of mRNAs were purchased from Nippon Shokubai Co., Ltd (Osaka, Japan) and Gene Design. The

DNA fragments were purchased from Gene Design and MilliporeSigma (Burlington, MA, USA).

#### Evaluation of translational activity of EGF mRNAs in HeLa cells

The translational activity of mRNAs was evaluated in HeLa cells. HeLa cells were cultured in DMEM medium supplemented with 10% FBS at 37 °C and 5% CO<sub>2</sub>. HeLa cells were seeded at 1.0 × 10<sup>4</sup> cells per well and cultured overnight. In the following day, old medium was removed and fresh Opti-MEM medium supplemented with 1% (v/v) BSA was added. mRNAs were mixed with 0.3% Lipofectamine MessengerMAX Transfection Reagent (Thermo Fisher Scientific) and added to HeLa cells. At each time point, the supernatant was collected and fresh Opti-MEM medium supplemented with 1% (v/v) BSA was added. The EGF concentration in the supernatant was evaluated using the AlphaLISA Human EGF immunoassay kit (Revvity, Waltham, MA, USA) according to the manufacturer's protocol. Data processing and statistical analyses were conducted using the GraphPad Prism software (GraphPad Software Inc., La Jolla, CA, USA).

#### Mice

All animal studies were conducted under the "Standards for Proper Conduct of Animal Experiments" established by Kyowa Kirin Co., Ltd, and received approval from the company's Institutional Animal Care and Use Committee (approval no: AN00043-Z01-24). Kyowa Kirin Co., Ltd is accredited by the Association for Assessment and Accreditation of Laboratory Animal Care International (AAALAC). Five-week-old male BALB/cAJcl mice were purchased from CREA Japan (Tokyo, Japan).

#### Evaluation of translational activity of EGF mRNAs *in vivo*

The mRNA samples were administered intradermally using a needle syringe or an Actranza® lab. i.d. delivery device (Daicel Corporation, Osaka, Japan). The mice were euthanized under anesthesia at 4, 96, and 168 h after administration. Skin samples were harvested, immediately frozen in liquid nitrogen, and homogenized using a ShakeMaster Neo (Bio Medical Science Inc., Tokyo, Japan). The crushed samples were resuspended in d-PBS(−) containing a protease inhibitor. At 4 °C, the samples were centrifuged at 9100 × g for 10 min. After centrifugation, the supernatant was collected and designated as the *in vivo* lysate. The concentration of hEGF protein in the lysate was quantified using the AlphaLISA Human EGF Immunoassay Kit (Revvity) according to the manufacturer's instructions. A calibration curve was constructed using Recombinant Human EGF GMP Protein, CF (R&D Systems, Minneapolis, MN, USA) diluted in d-PBS(−).

#### Delivery of firefly luciferase mRNA *in vivo*

Imaging analysis for the expression of 10 or 30 μg per head CleanCap® Fluc mRNA (5moU) (TriLink, San Diego, CA, USA) after a single intradermal administration was performed using the IVIS system (PerkinElmer, Waltham, MA, USA). The mice were imaged 4 h after administration of either N&S or Pyro.



Mice were anesthetized with isoflurane and subcutaneously injected with 3 mg per head VivoGlo™ Luciferin, *In Vivo* Grade (Promega) 15 min before imaging.

## Conclusions

This study comprehensively evaluated the effect of chemical modifications on the poly(A) tail of mRNA, particularly at high modification rates. Among them, PS, 2'-OMe, and 2'-MOE modifications dramatically enhanced mRNA stability against CAF1, whereas only PS maintained PABP binding at a modification rate of approximately 50%. Beyond the PS modification, combined modification of the poly(A) tail with 2'-F, 2'-OMe, and 2'-MOE significantly increased mRNA resistance to both CAF1 and nucleases in mouse skin lysates. Although 2'-F, 2'-OMe, and 2'-MOE modifications obstructed PABP binding, a poly(A) tail with this combinational modification regained PABP binding activity after the insertion of a 12-nt unmodified poly(A) upstream of the modified poly(A) sequence, even at a 100% modification rate in the 28-nt poly(A) sequence at the 3'-end. Importantly, the resulting poly(A) formulation significantly prolonged protein translation in cultured cells and mouse skin when applied to EGF mRNA. Although the transient protein expression profile remains a major obstacle to the widespread application of mRNA therapeutics, our findings offer a promising solution to this challenge.

## Author contributions

Atsushi Hashimoto: conceptualization, investigation, visualization, writing – original draft. Yuma Kunitomo: investigation, visualization, writing – original draft. Ittoku Kikuchi: investigation, visualization. Hiroki Yamada: investigation, writing – review & editing. Keiko Kobayashi: investigation. Kazuhiro Soshiroda: investigation. Hiromi Aman: investigation. Yasuaki Kimura: writing – review & editing, supervision. Yasuhisa Shiraishi: writing – review & editing, supervision. Satoshi Uchida: writing – review & editing, supervision. Hiroshi Abe: writing – review & editing, supervision. Junichiro Yamamoto: writing – review & editing, project administration, supervision. Hiroto Iwai: conceptualization, writing – review & editing, project administration, supervision.

## Conflicts of interest

AH, YK, IK, HY, KK, KS, HA, YS, JY, and HI are employees of Kyowa Kirin Co. Ltd.

## Data availability

The data supporting this study are included in the SI. See DOI: <https://doi.org/10.1039/d5cb00137d>

## Acknowledgements

This work was funded by Kyowa Kirin Co. Ltd.

## Notes and references

- U. Sahin, K. Karikó and Ö. Türeci, *Nat. Rev. Drug Discovery*, 2014, **13**, 759–780.
- Y. Weng, C. Li, T. Yang, B. Hu, M. Zhang, S. Guo, H. Xiao, X. J. Liang and Y. Huang, *Biotechnol. Adv.*, 2020, **40**, 107534.
- E. Rohner, R. Yang, K. S. Foo, A. Goedel and K. R. Chien, *Nat. Biotechnol.*, 2022, **40**, 1586–1600.
- C. Y. Chen, D. M. Tran, A. Cavedon, X. Cai, R. Rajendran, M. J. Lyle, P. G. V. Martini and C. H. Miao, *Mol. Ther. Nucleic Acids*, 2020, **20**, 534–544.
- D. Strzelecka, M. Smietanski, P. J. Sikorski, M. Warminski, J. Kowalska and J. Jemielity, *RNA*, 2020, **26**, 1815–1837.
- A. Aditham, H. Shi, J. Guo, H. Zeng, Y. Zhou, S. D. Wade, J. Huang, J. Liu and X. Wang, *ACS Chem. Biol.*, 2022, **17**, 3352–3366.
- J. Gorski, M. R. Morrison, C. G. Merkel and J. B. Lingrel, *Nature*, 1975, **253**, 749–751.
- A. O. Subtelny, S. W. Eichhorn, G. R. Chen, H. Sive and D. P. Bartel, *Nature*, 2014, **508**, 66–71.
- J. Lim, M. Lee, A. Son, H. Chang and V. N. Kim, *Genes Dev.*, 2016, **30**, 1671–1682.
- J. B. Rodriguez-Molina and M. Turtola, *FEBS Open Bio*, 2023, **13**, 1140–1153.
- R. Sawazaki, S. Imai, M. Yokogawa, N. Hosoda, S. I. Hoshino, M. Mio, K. Mio, I. Shimada and M. Osawa, *Sci. Rep.*, 2018, **8**, 1455.
- D. A. Mangus, M. C. Evans and A. Jacobson, *Genome Biol.*, 2003, **4**, 223.
- Q. Vicens, J. S. Kieft and O. S. Rissland, *Mol. Cell*, 2018, **72**, 805–812.
- A. M. Borman, Y. M. Michel and K. M. Kean, *Nucleic Acids Res.*, 2000, **28**, 4068–4075.
- B. Kim, J. Seol, Y. K. Kim and J. B. Lee, *Exp. Mol. Med.*, 2023, **55**, 283–289.
- T. Preiss and M. W. Hentze, *Nature*, 1998, **392**, 516–520.
- H. Chen, D. Liu, J. Guo, A. Aditham, Y. Zhou, J. Tian, S. Luo, J. Ren, A. Hsu, J. Huang, F. Kostas, M. Wu, D. R. Liu and X. Wang, *Nat. Biotechnol.*, 2025, **43**, 194–203.
- L. K. McKenzie, R. El-Khoury, J. D. Thorpe, M. J. Damha and M. Hollenstein, *Chem. Soc. Rev.*, 2021, **50**, 5126–5164.
- M. Egli and M. Manoharan, *Nucleic Acids Res.*, 2023, **51**, 2529–2573.
- M. Takahashi, N. Minakawa and A. Matsuda, *Nucleic Acids Res.*, 2009, **37**, 1353–1362.
- O. Perzanowska, M. Smietanski, J. Jemielity and J. Kowalska, *Chemistry*, 2022, **28**, e202201115.
- H. Yi, J. Park, M. Ha, J. Lim, H. Chang and V. N. Kim, *Mol. Cell*, 2018, **70**, 1081–1088e1085.
- A. P. Petit, L. Wohlböld, P. Bawankar, E. Huntzinger, S. Schmidt, E. Izaurrealde and O. Weichenrieder, *Nucleic Acids Res.*, 2012, **40**, 11058–11072.



24 M. Maryati, I. Kaur, G. P. Jadhav, L. Olotu-Umoren, B. Oveh, L. Hashmi, P. M. Fischer and G. S. Winkler, *Nucleic Acids Res.*, 2014, **42**, e30.

25 Y. Chen, E. Khazina, E. Izaurrealde and O. Weichenrieder, *Nucleic Acids Res.*, 2021, **49**, 6489–6510.

26 B. Stupler, C. Birck, B. Séraphin and F. Mauxion, *Nat. Commun.*, 2016, **7**, 10811.

27 A. Kahvejian, Y. V. Svitkin, R. Sukarieh, M. N. M'Boutchou and N. Sonenberg, *Genes Dev.*, 2005, **19**, 104–113.

28 J. Gao, Y. D. Tang, W. Hu and C. Zheng, *J. Virol.*, 2022, **96**, e0013622.

29 D. R. Gallie, *Translation*, 2014, **2**, e959378.

30 T. Sagae, M. Yokogawa, R. Sawazaki, Y. Ishii, N. Hosoda, S. I. Hoshino, S. Imai, I. Shimada and M. Osawa, *J. Biol. Chem.*, 2022, **298**, 101844.

31 A. H. Krotz, R. C. Mehta and G. E. Hardee, *J. Pharm. Sci.*, 2005, **94**, 341–352.

32 L. Wu, D. E. White, C. Ye, F. G. Vogt, G. J. Terfloth and H. Matsuhashi, *J. Mass Spectrom.*, 2012, **47**, 836–844.

33 H. Iwai, Y. Kimura, M. Honma, K. Nakamoto, K. Motosawa, T. Atago, K. Asano, F. Hashiya, N. Abe, K. Kobayashi, R. Ogisu, A. Hashimoto, K. Hiraishi, S. Saito, J. Yamamoto and H. Abe, *ChemRxiv*, 2024, preprint, DOI: [10.26434/chemrxiv-2024-bpx6](https://doi.org/10.26434/chemrxiv-2024-bpx6).

34 H. Yamada, H. Iwai, F. Hashiya, Y. Kimura, H. Abe and J. Yamamoto, *ChemBioChem*, 2025, **26**, e202400711.

35 N. L. Garneau, J. Wilusz and C. J. Wilusz, *Nat. Rev. Mol. Cell Biol.*, 2007, **8**, 113–126.

36 J. Probst, S. Brechtel, B. Scheel, I. Hoerr, G. Jung, H. G. Rammensee and S. Pascolo, *Genet. Vaccines Ther.*, 2006, **4**, 4.

37 R. C. Deo, J. B. Bonanno, N. Sonenberg and S. K. Burley, *Cell*, 1999, **98**, 835–845.

38 M. Görlich, C. G. Burd and G. Dreyfuss, *Exp. Cell Res.*, 1994, **211**, 400–407.

39 F. Zeng and R. C. Harris, *Semin. Cell Dev. Biol.*, 2014, **28**, 2–11.

40 J. Berlanga-Acosta, J. Gavilondo-Cowley, P. López-Saura, T. González-López, M. D. Castro-Santana, E. López-Mola, G. Guillén-Nieto and L. Herrera-Martínez, *Int. Wound J.*, 2009, **6**, 331–346.

41 X. Tang, H. Liu, S. Yang, Z. Li, J. Zhong and R. Fang, *Mediators Inflammation*, 2016, **2016**, 1927348.

42 Y. S. Kim, D. H. Lew, K. C. Tark, D. K. Rah and J. P. Hong, *J. Korean Med. Sci.*, 2010, **25**, 589–596.

43 M. N. Tabrizi, C. Chams-Davatchi, N. Esmaeli, P. Noormohammadpoor, F. Safar, H. Etemadzadeh, H. A. Ettehadi and F. Gorouhi, *J. Eur. Acad. Dermatol. Venereol.*, 2007, **21**, 79–84.

44 K. Y. Chan, T. D. Lindquist, M. J. Edenfield, M. A. Nicolson and A. R. Banks, *Invest. Ophthalmol. Visual Sci.*, 1991, **32**, 3209–3215.

45 C.-H. Yang, Y.-B. Huang, P.-C. Wu and Y.-H. Tsai, *Process Biochem.*, 2005, **40**, 1661–1665.

46 N. Abe, A. Imaeda, M. Inagaki, Z. Li, D. Kawaguchi, K. Onda, Y. Nakashima, S. Uchida, F. Hashiya, Y. Kimura and H. Abe, *ACS Chem. Biol.*, 2022, **17**, 1308–1314.

47 D. D. Kang, H. Li and Y. Dong, *Adv. Drug Delivery Rev.*, 2023, **199**, 114961.

48 D. Kawaguchi, A. Kodama, N. Abe, K. Takeuchi, F. Hashiya, F. Tomoike, K. Nakamoto, Y. Kimura, Y. Shimizu and H. Abe, *Angew. Chem., Int. Ed.*, 2020, **59**, 17403–17407.

49 J. Hertler, K. Slama, B. Schober, Z. Özrendeci, V. Marchand, Y. Motorin and M. Helm, *Nucleic Acids Res.*, 2022, **50**, e115.

50 S. Abbasi, M. Matsui-Masai, F. Yasui, A. Hayashi, T. A. Tockary, Y. Mochida, S. Akinaga, M. Kohara, K. Kataoka and S. Uchida, *Mol. Ther.*, 2024, **32**, 1266–1283.

51 L. Carlsson, J. C. Clarke, C. Yen, F. Gregoire, T. Albery, M. Billger, A.-C. Egnell, L.-M. Gan, K. Jennbacken, E. Johansson, G. Linhardt, S. Martinsson, M. W. Sadiq, N. Witman, Q.-D. Wang, C.-H. Chen, Y.-P. Wang, S. Lin, B. Ticho, P. C. H. Hsieh, K. R. Chien and R. Fritzsche-Danielson, *Mol. Ther.-Methods Clin. Dev.*, 2018, **9**, 330–346.

